

The giant star forming halo associated with the radio galaxy PKS1932-46.*

M. Villar-Martín^{1†}, C. Tadhunter², R. Morganti³, J. Holt²

¹*Instituto de Astrofísica de Andalucía (CSIC), Aptdo. 3004, 18080 Granada, Spain*

²*Dept. of Physics and Astronomy, University of Sheffield, Sheffield S3 7RH, UK*

³*ASTRON, PO Box 2, 7990 Dwingeloo, the Netherlands*

ABSTRACT

We report the discovery of a giant (~ 160 kpc) knotty extended emission line nebula associated with the radio galaxy PKS1932-46 at $z = 0.23$. The 2-d long slit spectra, obtained with VLT-FORS2 at a large angle ($\sim 63^\circ$) to the radio source axis, shows that the nebula extends well beyond the radio structure and the ionization cones of the active nucleus. This is one of the largest ionized nebulae yet detected around a radio galaxy at any redshift. The analysis of the ionization, morphological and kinematic properties of the knots suggests that these are star forming objects, probably compact HII galaxies. We propose that the giant structure is a star forming halo associated with the debris of the merger that triggered the activity. This study reinforces the view that radio galaxies are activated by major mergers which also trigger substantial star formation. The star formation activity can extend on the scale of a galaxy group, beyond the old stellar halo of the host galaxy.

Key words: galaxies: active; galaxies:individual: PKS1932-46; galaxies: evolution

1 INTRODUCTION

Extended emission line haloes around radio galaxies have the potential to provide key information about the origins of the prodigious quasar and jet activity and how these objects are related to the evolution of giant elliptical galaxies (e.g. Baum & Heckman 1989). However, in order to use the emission lines in this way it is essential to distinguish the intrinsic properties of the warm ISM in the host galaxies/groups from the effects of the AGN/jet activity. Unfortunately, most previous long-slit spectroscopic studies have focussed on the high surface brightness extended emission line regions (EELR) that are frequently aligned with the radio axis (Baum & Heckman 1989). Such structures are often dominated by jet-induced shocks (Clark et al. 1997, Villar-Martín et al. 1999, Best, Röttgering & Longair 2000) and it is difficult to determine the intrinsic properties of the ISM.

Here we report observations of a spectacular emission line nebula in the FR II radio galaxy PKS1932-46 ($z = 0.23$) that extends well beyond the radio structures and ionization cones associated with the nuclear activity, and allows us to investigate the properties of the undisturbed ISM in the extended halo around the host galaxy.

Early spectroscopic observations of PKS1932-46 re-

vealed an emission line nebulosity with a rich emission line spectrum extending out to a radius of $23''$ (~ 92 kpc) along the radio axis¹ (Villar-Martín et al. 1998, VM98 hereafter). The object is surrounded by shell, filament and knot type structures (VM98) that are typical of interacting systems.

All spectroscopic studies previously published of PKS1932-46 were based on shallower long slit spectra taken along the radio axis. We present here deep optical VLT-FORS2 spectroscopy with the slit at PA-9, misaligned by $\sim 63^\circ$ relative to the radio axis (PA-72). The observations and data reduction process are described in §2. The main results are described in §3 and the discussion and conclusions are presented in §4.

2 OBSERVATIONS

Deep blue and red spectra were obtained using the FORS2 spectrograph on VLT (ESO-Paranal Observatory) on 24th Sept 2003. The log of the observations is presented in Table 1. The data were reduced following standard procedures with STARLINK, IRAF and FIGARO packages. The spectra were debiased, flat fielded, wavelength and flux calibrated, combined and cosmic ray removed, background

* Based on observations carried out at the European Southern Observatory, Paranal, Chile with FORS2 on VLT (UT1).
† email:montse@iaa.es

¹ We assume $\Omega_\Lambda = 0.7$, $\Omega_M = 0.3$, $H_0 = 65 \text{ km s}^{-1} \text{ Mpc}^{-1}$. In this Cosmology, 1 arcsec = 4.0 kpc

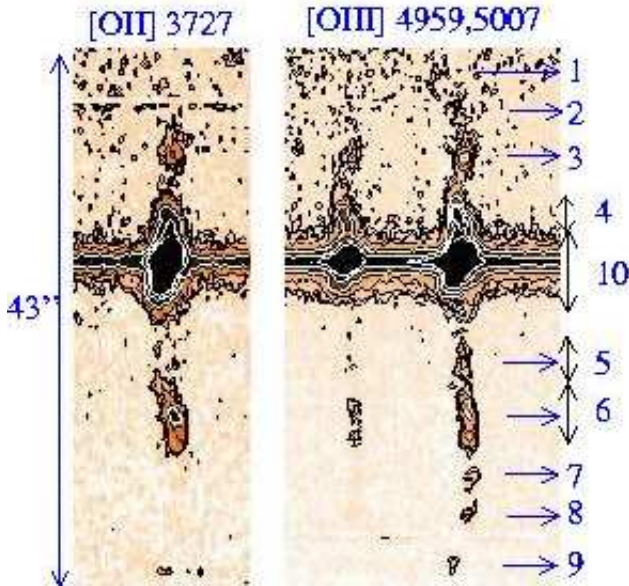


Figure 1. PKS1932-46: 2D spectra of the [OIII] and [OII] lines along PA -9° . A spectacular extended region of ionized gas is detected along $\sim 40''$ (~ 160 kpc). It consists of a series of knots some of which are spatially unresolved. The apertures used in the analysis presented in this paper are indicated.

subtracted, corrected for geometrical distortion and atmospheric absorption features. Comparison of several spectrophotometric standard stars taken with a $5''$ slit throughout the run gave a relative flux calibration accuracy of 5 per cent over the entire spectral range of the observations. The two resulting spectra (blue and red) were aligned spatially using the continuum centroids.

1D spectra were extracted from several apertures (ap. hereafter) shown in Fig. 1, which were selected to isolate individual knots (in most cases) along the slit. A pixel by pixel analysis was performed in the $r \lesssim 2''$ region (ap.10, Fig. 1). As an example, the spectra of ap. 4 and 6 are shown in Fig. 2.

The line profiles were fitted with Gaussian functions, which in general are a good representation of the bulk of the line profiles. The FWHM of the lines were corrected for the instrumental profile (IP, Table 1) in quadrature. The velocity shift V_{sh} was calculated relative to the [OIII] $\lambda 5007$ central wavelength measured at the spatial position of the continuum centroid. The spatial variation of the FWHM and V_{sh} is shown in Fig. 3.

The seeing for the observations was $\sim 0.92 \pm 0.03''$, narrower than the $1.3''$ wide slit. Point sources do not fill the slit. This could significantly affect especially the kinematic measurements of the compact knots (e.g. Villar-Martín et al. 2003). Since the narrowness of the lines emitted by the knots has an important impact on our conclusions (see §3), we have been conservative and assumed for the knots the minimum possible value of the IP, i.e., that of a point source (~ 6.1 Å). Since some of the knots are spatially resolved, it is clear that the upper limits shown in Fig. 3 are very conservative.

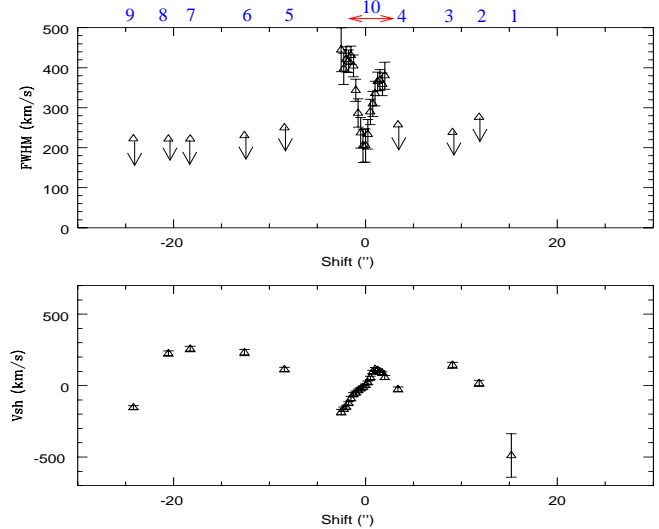


Figure 3. Spatial variation along the slit of the FWHM and velocity shift of [OIII] $\lambda 5007$. The numbers above the top panel indicate the aperture nr. (see Fig. 1). FWHM values for aperture 1 are not shown due to the noise. The upper limits for the FWHM are very conservative values (see text).

3 RESULTS

Fig. 1 clearly reveals a giant knotty emission line region that extends for $\sim 40''$ (~ 160 kpc), well beyond the radio structures (VM98). We have isolated three gaseous regions that differ in their kinematic properties.

- *The nuclear spectrum ($r < 1''$, inner ap.10).* This spectrum is typical of the narrow line region (NLR) of active galaxies. It presents strong high ionization lines ([NeV] $\lambda\lambda 3426, 3446$ and HeII $\lambda 4686$) as well as relatively strong low ionization lines ([NII] $\lambda\lambda 6548, 6583$, [OI] $\lambda 6300$, [OII] $\lambda 3727$, etc). The electron temperature measured using the [OIII] lines is very high with $T_e = 20000 \pm 700$ K.

Fits to the [OIII] line profiles, which have the highest S/N, demonstrate that the best fit is obtained with two Gaussians with FWHM 280 ± 20 km s $^{-1}$ and 1400 ± 200 km s $^{-1}$ respectively, with the broad component blueshifted by $\sim 150 \pm 100$ km s $^{-1}$ relative to the narrow component.

The same kinematic components also provide good fits to all the other emission lines (similar to the situation in Cygnus A, for example: see Taylor, Tadhunter & Robinson 2003), including the H α + [NII] blend (see Figure 4). In the latter case, the [OIII] model provides a good fit to the wings of the blend without the need for the additional broad component (FWHM ~ 2400 km s $^{-1}$) which led to the broad line radio galaxy (BLRG) classification of VM98. Therefore, in contrast to the conclusions of these authors, the spectral properties of the nuclear regions are fully consistent with PKS1932-46 being a narrow line radio galaxy (NLRG). Further evidence against the idea that this is a broad line radio galaxy is provided by near-IR spectroscopic observations which show no signs of broad wings to the P α line (Bellamy, private communication).

The measured H α /H β values are 3.8 ± 0.2 and 6 ± 2 for the narrow and the broad components respectively, implying significant reddening especially for the broad component.

- *The near nucleus ($1'' < r < 3-5''$, outer ap. 10 and*

Date	Instrument & Telescope	Grating	$\Delta\lambda^*$ Å	Exp. time sec	Slit PA (N to W)	IP Å	Slit width "	seeing "
24/09/2003	UT1+FORIS2	GIRIS_600B	3400-6030	3x900	-9°	6.5±0.2	1.3	~0.92±0.03
24/09/2003	UT1+FORIS2	GRIS_600RI	4950-8250	3x900	-9°	7.4±0.2	1.3	~0.92±0.03

Table 1. Log of the observations. (*Approximate useful spectral range)

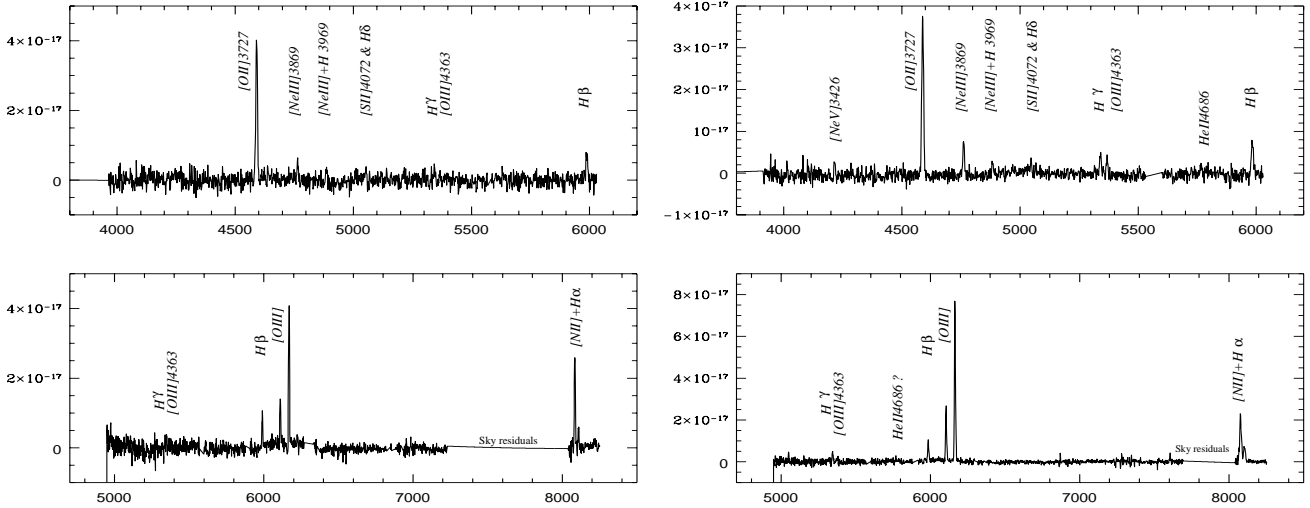


Figure 2. Blue and red spectra extracted from apertures 6 (left) and 4 (right).

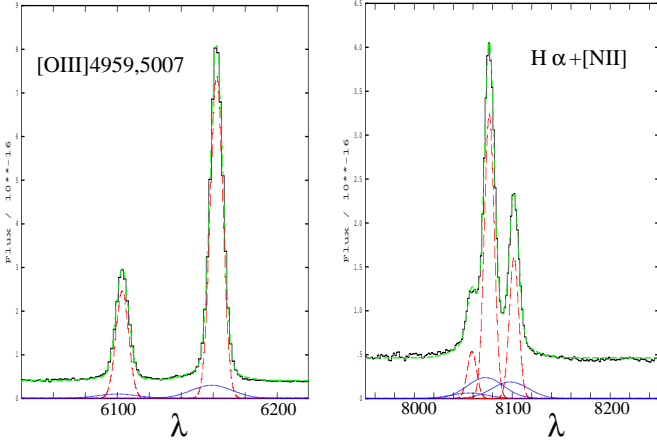


Figure 4. Fit to the [OIII] and H α + [NII] lines. The fit (dashed-green) and data (solid-black) are shown in each panel above the Gaussians of the individual kinematics components, which have been shifted down for clarity: narrow components (dashed-red) and broad components (solid-blue) (see the electronic edition of the Journal for a colour version of this figure). The same kinematic components found in the high S/N [OIII] lines provide good fits to the H α + [NII] blend (see text). This implies that PKS1932-46 is a NLRG, rather than a BLRG as previously thought.

ap. 4). The spectrum of the extended gas in the near-nuclear region is characteristic of active galaxies, with strong [NeV] λ 3426 and HeII λ 4686 and low ionization lines (see Fig. 2). High electron temperatures are also measured with T_e in the range 20000-24000 K in ap. 4 and the gas just outside the nuclear region. The measured H α /H β = 3.1±0.2 is consistent with the case B value.

The gas in this region shows complex kinematics with broad lines compared with the nuclear region (see Fig. 3) and two split narrow components in aperture 4 (the emission in ap. 4 can be resolved into two apparently spatially unresolved knots). These are shifted in velocity by 230 ± 30 km s $^{-1}$ and have FWHM([OIII] λ 5007) = 220 ± 40 and $\lesssim 200$ km s $^{-1}$ respectively. The integrated spectrum of aperture 4 shows an apparent anti-correlation between line width and ionization level, similar to that found in other radio galaxies with clear signs of jet-gas interactions (Clark et al. 1997, Villar-Martín et al 1999). The [OIII] doublet lines have FWHM= 280 ± 20 km s $^{-1}$ and FWHM of [NeV] λ 3426 ≤ 250 km s $^{-1}$. On the other hand, low ionization lines such as [NII], [OII] and the Balmer lines have similar widths (FWHM= 400 - 530 km s $^{-1}$) within the errors. Complex kinematics is also obvious in the 2D image of the long-slit spectrum in the H α + [NII] region, with each line consisting of two kinematic components. This kinematically perturbed region is about the same size as the width of the radio cocoon in the direction perpendicular to the radio axis (VM98). The kinematic and ionization properties of this gas are therefore likely to be strongly affected by shocks induced by the interaction between the gas and the radio structures.

- *The extended halo ($r > 5''$, ap. 5 to 9).* This gas shows an irregular knotty morphology. The total extension is striking ($\sim 40''$ or ~ 160 kpc). The individual knots have sizes of $\lesssim 10$ kpc (the emission within aperture 6 can be resolved into two different knots of spatial FWHM $\sim 1.4''$ and $2.0''$ respectively). The lines (FWHM $\lesssim 250$ km s $^{-1}$) are most probably narrower than in the inner regions (see §2). The smoothness and symmetry of the velocity curve defined by the knots

suggest that all of them follow a common kinematic pattern, which is decoupled from the gas at $r \lesssim 5''$ (Fig. 3).

The Balmer decrement was measured in ap. 3 and 6, giving $H\alpha/H\beta = 2.7 \pm 0.5$ and 3.2 ± 0.3 respectively, consistent with the case B value within the errors.

We show in Fig. 5 three diagnostic diagrams involving the main emission lines that could be detected in most apertures across the extended halo. We have also included ap. 4 (discussed above), the integrated nuclear spectrum and the gas extended *along the radio axis* discussed by VM98 (inner and outer EELR). For comparison, the standard solar metallicity power-law (index $\alpha = -1.5$), single slab photoionization model sequence often applied to low redshift active galaxies (e.g. Robinson et al. 1987) is also shown. The ionization parameter U varies along the sequence (models with $\log U = -3, -2, -1$ are marked). The position of a sample of HII galaxies extracted from the catalogue by Terlevich et al. (1991) is also shown. The diagrams show that the ionization properties of the knots vary along the slit. The main results are:

- Ap. 3, 4 and 5 and the nuclear spectrum (open symbols) lie close to the AGN photoionization models. The different positions of the knots can be naturally explained by a decrease in the ionization level with increasing distance from the AGN: ap. 3 and 5 (which are located at similar distance (8–10'' from the AGN) show similar ionization level, while the gas in ap. 4 ($\sim 3.5''$ from the AGN) has higher ionization level. As discussed above, it is also possible that the gas in ap. 4 (see above) is partially ionized by shocks.

The outer EELR (VM98) is gas located at $\sim 20''$ *along the radio axis* and just beyond the Eastern radio lobe. It follows the same U sequence discussed above and presents the highest ionization level. Since it is apparently located at a much larger distance than ap. 3 to 5 ($r < 10''$), this suggests a change in the physical conditions (lower density) or that the AGN continuum is stronger along the radio axis (see §4).

- Ap. 6 shows a mixed spectrum. The [NII] emission places it in the area of the star forming objects while the oxygen lines place it closer to the AGN models.

- The outer apertures (2, 7 and 8+9) show a spectrum characteristic of star forming objects. The three apertures have very similar [OIII]/ $H\beta \sim 3$ –3.5.

It seems therefore, that there is a gradual change on the balance of the ionization mechanism when we move outwards along the slit. AGN related processes dominate in the inner regions ($r \lesssim 8''$ or ap. 3, 4, 10 and 5). A mixture of stellar and AGN photoionization is then apparent at intermediate distances ($\sim 13''$, ap. 6) and at larger distances the objects are ionized by stars (ap. 2, 7, 8, 9).

The $H\beta$ luminosities of the outer knots (2, 7, 8, 9) are $\sim 1\text{--}2 \times 10^{39}$ erg s $^{-1}$, a factor between ~ 2 and 10 times lower than the more interior knots, and within the range of values measured in HII galaxies (Terlevich et al. 1991). The implied star forming rates are $\sim 0.02\text{--}0.05$ M_{\odot} yr $^{-1}$, ignoring underlying line absorption and reddening (Kennicutt 1998). Their compact appearance, small sizes ($\lesssim 10$ kpc) and narrow emission lines ($\text{FWHM} \lesssim 250$ km s $^{-1}$) are all consistent with values measured in compact HII galaxies (e.g. Terlevich et al. 1991, Guzmán et al 1997). Continuum is detected from ap. 8 (and maybe 9 as well), although its nature is not known

(nebular or stellar). The non detection of continuum in ap. 2 and 7 does not contradict the stellar interpretation, since large $H\beta$ equivalent widths (> 100 Å rest frame) are expected for young stellar ages (\lesssim few Myr) (e.g. Stasinska, Schaerer & Leitherer 2001) which would imply continuum levels well under the detection limit. The [OII], [OIII] and $H\beta$ lines were used to estimate the oxygen abundance (Aller 1984) of apertures 2, 7 and 8+9. A T_e value of 12000 K was assumed (higher temperatures produce lower abundances). The derived abundances are $\sim 18\%$, $\lesssim 21\%$ and 15% (O/H) $_{\odot}$ for apertures 2, 7 and 8+9 respectively. Similar values are often derived for compact HII galaxies (e.g. Terlevich et al. 1991).

All properties of the outer knots studied here are therefore consistent with compact HII galaxies. Although the spectra of the inner knots (ap. 3 to 6) are distorted by AGN related processes, their compact appearance, small sizes ($\lesssim 10$ kpc) and narrow emission lines ($\text{FWHM} \lesssim 250$ km s $^{-1}$) are also consistent with values measured in compact HII galaxies. Therefore, we propose that *all the knots (ap. 2 to 9)* in the giant halo are star forming objects

4 DISCUSSION AND CONCLUSIONS

We have discovered a giant gaseous knotty structure that extends for a striking distance of ~ 160 kpc. This is one of the largest emission line halos ever detected around an active galaxy at any redshift. We have proposed that the halo comprises of star forming objects, probably compact HII galaxies.

Based on continuum properties, young stellar populations (YSP) have been detected in the nuclear regions of a significant fraction of nearby radio galaxies (e.g. Tadhunter et al. 2002, 2005). However, most of these YSP represent relatively old post-starburst populations (0.05–2 Gyr). Our new observations show that the star formation is ongoing in PKS1932–46 and it can actually spread over spatial scales of more than 100 kpc. Since the object lies in a rich environment where a merger/interaction event is likely to be taking place (VM98), we propose that the giant halo is a residual feature of such process where compact star forming objects have formed. Morphologically, the giant halo reminds us of the linear knotty ionized structure extended for \gtrsim tens of kpc associated with the system IC 1182, which shows clear signs of interactions and/or mergers (e.g. Moles et al. 2004). The authors propose that some of the $H\alpha$ condensations found in the large scale tails could be tidal dwarf proto-galaxies. The existence of isolated intergalactic HII regions has also been reported at ~ 100 kpc from the early type galaxy NGC1490 (Oosterloo et al. 2004). The HII regions are associated with large HI clouds lying along a 500 kpc long arc, which is likely to be a product of tidal interactions or merger events.

Giant kinematically unperturbed halos ($\gtrsim 100$ kpc) of ionized gas have been found in some high redshift radio galaxies ($z \sim 2.5$, e.g. Villar-Martín et al. 2003). Unfortunately, the slit was always located along the radio axis and the observed properties are strongly distorted by the nuclear activity. It is interesting to consider whether the giant halo discovered around PKS1932–46 has a similar nature. The detailed study presented here opens the possibility that the high redshift halos are also giant star forming regions, the product of ongoing merger events. Star formation across gi-

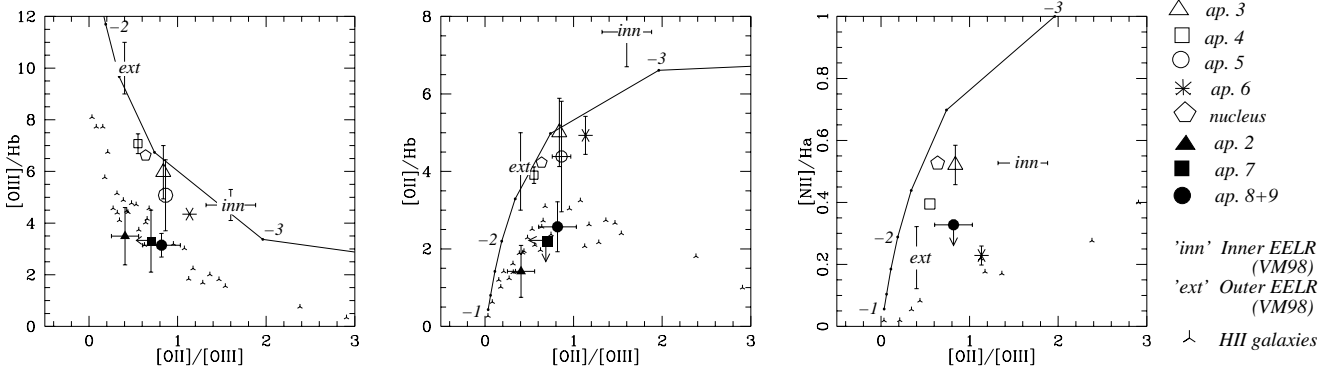


Figure 5. Diagnostic diagrams showing the position of all apertures where the main lines could be measured. The standard power law ($\alpha=-1.5$) ionization parameter U sequence often applied to radio galaxies is shown as a solid black line (Robinson et al. 1987). The negative numbers mark $\log(U)$. A sample of HII galaxies are also plotted (Terlevich et al. 1991), as well as the line ratios measured in the extended gas along the radio axis by VM98 (*inn* and *ext*). Errorbars smaller than the symbols size are not shown. $[\text{NII}]/\text{H}\alpha$ could not be measured for ap. 2 and 5. The gas within ap. 3, 4 and 5 (open symbols) is likely to be mostly ionized by AGN related processes. Moving outward along the slit, ap. 6 (star symbol) shows mixed properties between AGNs (left and middle panels) and star forming galaxies (right panel). The outer knots (ap. 2, 7 and 8+9, solid symbols) have spectroscopic properties consistent with HII galaxies. There is therefore a gradual change on the ionization mechanism along the slit such that stellar ionization becomes dominant in the outer knots.

ant spatial scales (several tens of kpc to 1 Mpc) has been reported for several radio galaxies at $z \sim 2-4$ (Stevens et al. 2003) based on sub-mm observations.

We have concluded that AGN photoionization is likely to excite the gas in the knots located closer to the nucleus (ap. 3, 4, 5). Jet-induced shocks could also play a role in ap.4 (see §3). The slit was placed at -9° , shifted by $\sim 63^\circ$ relative to the radio axis. In the simplest scenario, the radio axis is also the axis of the ionization cones, which are expected to have an opening angle of 90° (Barthel 1989). In such case, and given that PKS1932-46 is a NLRG (see §3) the slit position is outside the ionization cones. A misalignment of $\gtrsim 15^\circ$ between the radio axis and the cones axis is required for AGN photoionization to be plausible. Otherwise we need to invoke larger cone opening angles, or the existence of a porous torus that allows some filtered continuum to escape in directions outside the standard 90° cones.

Overall, this study reinforces the view that the nuclear activity in radio galaxies is triggered by major galaxy mergers and there is substantial associated star formation (e.g. Heckman et al. 1986), which can extend on the scale of a galaxy group, beyond the old stellar halo of the host galaxy.

ACKNOWLEDGMENTS

We thank the staff on Paranal for their support. MVM is supported by the Spanish National program Ramón y Cajal. JH acknowledges support from a PPARC studentship. We thank the referee Andy Robinson for useful comments.

REFERENCES

- Aller L. H., 1984, *Physics of Thermal Gaseous Nebulae*, D. Reidel, Publ. Company, Dordrecht
- Baum S. A. Heckman T., 1989, *ApJ*, 336, 702
- Best P., Röttgering H., Longair M., 2000, *MNRAS*, 311, 23
- Barthel P., 1989, *ApJ*, 336, 606
- Clark N.E., Tadhunter C.N., Morganti R., Killeen N.E.B., Fosbury R.A.E., Hook R.N., Siebert J., Shaw M. A., 1997, *MNRAS*, 286, 558
- Guzmán R. Gallego J., Koo D., Philips A., Lowenthal J., Faber S., Illingworth G., Vogt N., 1997, *ApJ*, 489, 559
- Heckman T. M., Smith E. P., Baum S. A., van Breugel W., Miley G., Illingworth G. D., Bothun G. D., Balick G. D., 1986, *ApJ*, 311, 526
- Kennicutt R.C., ARA&A, 36, 189
- Moles M., Bettoni D., Fasano G., Kjargaard P., Varela J., Milvang-Jensen B., 2004, *A&A*, 418, 495
- Oosterloo T., Morganti R., Sadler E., Ferguson A., van der Hulst T., Jerjen H., IAU Symp. no. 217, 2003 Sydney. Ed. P.A. Duc, J. Braine, and E. Brinks. San Francisco: Astronomical Society of the Pacific, 2004., p.486
- Robinson A., Binette L., Fosbury R. A. E., Tadhunter C., 1987, *MNRAS*, 227, 97
- Stasińska G., Schaerer D., Leitherer C., 2001, *A&A*, 370, 1
- Stevens J.A., Ivison R., Dunlop J., Smail I., Percival W., Hughes D.H., Röttgering H., van Breugel W., Reuland M., 2003, *Nature*, 425, 264
- Tadhunter C., Villar-Martín M., Morganti R., Bland-Hawthorn J., Axon D., 2000, *MNRAS*, 314, 849
- Tadhunter C., Dickson R., Morganti R., Robinson T., Wills K., Villar-Martín M., Hughes M., 2002, *MNRAS*, 330, 977
- Tadhunter C., Robinson T., González Delgado R., Wills K., Morganti R., 2005, *MNRAS*, 356, 480
- Taylor M. D., Tadhunter C., Robinson T., 2003, *MNRAS*, 342, 995
- Terlevich R., Melnick J., Masegosa J., Moles M., Copetti M., 1991, *A&AS*, 91, 285
- Villar-Martín M., Tadhunter C., Morganti R., Clark N., Killeen N., Axon D., 1998, *A&A*, 332, 479 (VM98)
- Villar-Martín M., Tadhunter C.N., Morganti R., Axon D., Koekemoer A., 1999, *MNRAS*, 307, 24
- Villar-Martín M., Vernet J., di Serego Alighieri S., Fosbury R., Humphrey A., Pentericci L., 2003, *MNRAS*, 346, 273